Title

Magnetic resonance imaging in Alzheimer's Disease Neuroimaging Initiative 2.

Journal

Alzheimer's & dementia : the journal of the Alzheimer's Association, 11(7)

ISSN

1552-5260

Authors

Jack, Clifford R
Barnes, Josephine
Bernstein, Matt A
et al.

Publication Date

2015-07-01

DOI

10.1016/j.jalz.2015.05.002

Peer reviewed

Alzheimer's & Dementia 11 (2015) 740-756

Magnetic resonance imaging in Alzheimer's Disease Neuroimaging Initiative 2

Clifford R. Jack, Jr.,[a,*], Josephine Barnes[b], Matt A. Bernstein[a], Bret J. Borowski[a], James Brewer[c], Shona Clegg[b], Anders M. Dale[c], Owen Carmichael[d], Christopher Ching[e], Charles DeCarli[d,f], Rahul S. Desikan[g], Christine Fennema-Notestine[g,h], Anders M. Fjell[i], Evan Fletcher[d,f], Nick C. Fox[b], Jeff Gunter[a], Boris A. Gutman[e], Dominic Holland[c], Xue Hua[e], Philip Insel[j], Kejal Kantarci[a], Ron J. Killiany[k], Gunnar Krueger[l], Kelvin K. Leung[m], Scott Mackin[j,n], Pauline Maillard[d,f], Ian B. Malone[b], Niklas Mattsson[o], Linda McEvoy[g], Marc Modat[b,m], Susanne Mueller[j,p], Rachel Nosheny[j,p], Sebastien Ourselin[b,m], Norbert Schuff[j,p], Matthew L. Senjem[a], Alix Simonson[j], Paul M. Thompson[e], Dan Rettmann[q], Prashanthi Vemuri[a], Kristine Walhovd[i], Yansong Zhao[r], Samantha Zuk[a], Michael Weiner[j,n,p,s,t]

[a]*Department of Radiology, Mayo Clinic, Rochester, MN, USA*
[b]*Department of Neurodegenerative Disease, Dementia Research Centre, Institute of Neurology, University College London, London, UK*
[c]*Department of Neuroscience, University of California at San Diego, La Jolla, CA, USA*
[d]*Department of Neurology, University of California at Davis, Davis, CA, USA*
[e]*Department of Neurology, Imaging Genetics Center, Institute for Neuroimaging & Informatics, University of Southern California, Marina del Rey, CA, USA*
[f]*Center for Neuroscience, University of California at Davis, Davis, CA, USA*
[g]*Department of Radiology, University of California at San Diego, La Jolla, CA, USA*
[h]*Department of Psychiatry, University of California at San Diego, La Jolla, CA, USA*
[i]*Department of Psychology, University of Oslo, Oslo, Norway*
[j]*Department of Radiology and Biomedical Imaging, Center for Imaging of Neurodegenerative Diseases, San Francisco Veterans Affairs Medical Center, San Francisco, CA, USA*
[k]*Department of Anatomy and Neurobiology, Boston University School of Medicine, Boston, MA, USA*
[l]*Siemens Medical Solutions, Boston, MA, USA*
[m]*Translational Imaging Group, Centre for Medical Image Computing, University College London, London, United Kingdom*
[n]*Department of Psychiatry, University of California at San Francisco, San Francisco, CA, USA*
[o]*Clinical Neurochemistry Laboratory, Institute of Neuroscience and Physiology, University of Gothenburg, Mölndal, Sweden*
[p]*Department of Radiology, University of California at San Francisco, San Francisco, CA, USA*
[q]*MR Applications and Workflow, GE Healthcare, Rochester, MN, USA*
[r]*Philips Healthcare, Cleveland, OH, USA*
[s]*Department of Medicine, University of California at San Francisco, San Francisco, CA, USA*
[t]*Department of Neurology, University of California at San Francisco, San Francisco, CA, USA*

Abstract

Introduction: Alzheimer's Disease Neuroimaging Initiative (ADNI) is now in its 10th year. The primary objective of the magnetic resonance imaging (MRI) core of ADNI has been to improve methods for clinical trials in Alzheimer's disease (AD) and related disorders.

Methods: We review the contributions of the MRI core from present and past cycles of ADNI (ADNI-1, -Grand Opportunity and -2). We also review plans for the future-ADNI-3.

Results: Contributions of the MRI core include creating standardized acquisition protocols and quality control methods; examining the effect of technical features of image acquisition and analysis on outcome metrics; deriving sample size estimates for future trials based on those outcomes; and

*Corresponding author. Tel.: +1-507-284-8548; Fax: +1-507-284-9778.

E-mail address: jack.clifford@mayo.edu

http://dx.doi.org/10.1016/j.jalz.2015.05.002

piloting the potential utility of MR perfusion, diffusion, and functional connectivity measures in multicenter clinical trials.

Discussion: Over the past decade the MRI core of ADNI has fulfilled its mandate of improving methods for clinical trials in AD and will continue to do so in the future.

Keywords: Alzheimer's disease; Alzheimer's Disease Neuroimaging Initiative; ADNI; Diffusion; MRI; Neuroimaging; Perfusion; Resting functional MRI

1. Introduction

The overarching objective for the Alzheimer's Disease Neuroimaging Initiative (ADNI) magnetic resonance imaging (MRI) core has been to improve methods for clinical trials in Alzheimer's disease (AD) and related disorders. Our approach has included the following elements: develop standardized MRI protocols; port these to all needed platforms of the three major MR vendors (GE, Siemens and Philips); qualify all scanners at baseline and requalify following upgrades; perform near real time quality control (QC); perform and post publicly, quantitative measurements that are relevant to AD clinical trials on all scans [1].

ADNI-1 focused primarily on structural MRI to study morphological changes associated with AD [1]. Although the ADNI cohort was recruited to study AD, not vascular disease, ADNI-1 included a T2/proton density sequence to ascertain incidental vascular changes. Subjects with hemispheric infarctions at baseline were excluded from ADNI-1, but white matter hyperintensities of any severity were not excluded. ADNI-GO/2 retained this focus on anatomic changes in AD but added a Fluid Attenuation Inversion Recovery (FLAIR) sequence to better depict cerebrovascular disease and also added a T2* gradient echo sequence for the detection of cerebral microbleeds (CMB) [2]. ADNI-GO/2 also added "experimental" sequences for perfusion MRI (arterial spin labeling, ASL), diffusion MRI (diffusion tensor imaging, DTI), and task-free functional MRI (TF-fMRI) also known as resting fMRI [3]. These sequences were selected because they are a major focus of modern imaging science (more so than anatomic MRI). Our thinking was that functional measures, particularly ASL and TF-fMRI, might be more sensitive to early disease-related effects than anatomic measures. A fourth experimental sequence was added after ADNI-GO/2 had begun—a high-resolution coronal T2 fast spin echo for the purpose of measuring hippocampal subfield volumes [4]. These "experimental" sequences were performed in a vendor-specific manner to pilot their potential use in multicenter clinical trials: DTI on GE systems; TF-fMRI on Philips systems; ASL; and coronal T2 on Siemens systems. Reasons for this approach were: (1) We used only vendor product sequences in ADNI-GO/2 (i.e. no works in progress sequences were used, because these require a research license for each site), and some of these sequences were not available as product from all MR vendors at the time ADNI-GO/2 began, and (2) implementation of these sequences was highly variable across vendors. To optimize the uniformity of acquisition we limited each of these sequences to a single vendor [3].

This report is divided into two major sections—the first outlines contributions of the ADNI MRI core to date (i.e. ADNI-1, GO/2) and the second outlines plans for ADNI 3.

2. Accomplishments of the ADNI-MRI core to date

2.1. Technical standards

A major goal of ADNI-MRI was the standardization of imaging methods to facilitate MRI in clinical trials. Ideally, variation in quantitative measures across subjects and over time should be a product of disease effects, not due to nonuniform imaging methods. To achieve the goal of standardized acquisitions across all scanners and across time, protocols were developed that were compatible with a variety of hardware/software configurations within each of the three major MRI vendors' product lines [1]. A total of 59 3T systems and 40 1.5T scanners have been qualified and requalified over time as needed with upgrades. This resulted in a large infrastructure of harmonized MRI scanners at ADNI sites which have been used in various clinical trials in AD and related disorders. Vendor- and version-specific protocols are publically posted which resulted in the wide use of the ADNI-MRI protocols both by the pharmaceutical industry and academic entities.

ADNI methods also include near real-time QC of all examinations. QC results are used within ADNI to identify subjects who may have medical problems, to select subjects with failed examinations for rescans, and to label the quality of scans for analysis purposes. QC was managed by the Mayo group. Once uploaded, every MR study was examined by a fully automated software program created at Mayo to check tens of imaging parameters in each image file against the protocol standard (which was specific for vendor/scanner model/software version). Scans were also viewed and graded manually by a MR technologist to ascertain quality problems such as motion artifact and also potential medical findings. Scans that failed protocol checking or visual quality prompted a rescan. All scans with potential medical findings were reviewed by MDs (CRJ or KK) at Mayo.

The ADNI phantom was designed at the beginning of ADNI-1 to address the need for a high-resolution three-dimensional (3D) geometric phantom for quantitative structural MRI. The ADNI phantom was initially used to correct for changes in scanner geometric scaling over time, scanner

qualification, and ongoing scanner QC [5]. The ADNI phantom was also adopted for assessing scanner performance by other multisite studies (e.g., Systolic Blood Pressure Intervention Trial: Memory and Cognition in Decreased Hypertension, Atherosclerosis Risk in Communities, Dominantly Inherited Alzheimer Network, and AddNeuroMed) [6]. The ADNI phantom was designed to correct several imaging artifacts and some of these were addressed later by improved vendor products. This is described in more detail in the following section. Consequently, ADNI now uses this phantom only for scanner qualification and requalification. A separate phantom scan is no longer acquired with each patient examination [3]. The success of the ADNI phantom, however, raised awareness in the MR community about the need for a high-resolution 3D geometric phantom for quantitative structural MRI. This led the International Society of Magnetic Resonance in Medicine (ISMRM) Committee on Quantitative MRI along with the National Institute of Technology Standards (NIST) to design the NIST-ISMRM MRI System Phantom [7]. The NIST-ISMRM system phantom [7] uses the ADNI phantom design for geometric fidelity but also incorporates additional elements. It also addresses issues identified over the years of phantom use in ADNI including enhanced physical robustness.

2.2. Image postprocessing

The state of the MRI field when ADNI-1 was launched in 2004 raised concerns about, (1) the stability of geometric scaling over time, (2) image intensity nonuniformity, and (3) geometric warping. All these effects can add noise/error to quantitative anatomic measures and thus correcting these should improve measurement precision. Offline postprocessing corrections addressing each of these three issues were therefore instituted in ADNI-1 [1]. When ADNI-1 began, the MRI field had begun moving away from single channel transmit/receive head coils, which have relatively uniform intensity profiles, to multiarray receive-only head coils which do not. Studies by the ADNI-MRI core showed that standard artifact-correction methods could be improved on and optimized for multiarray receiver coils. To correct for the inherent intensity nonuniformity in the multiarray receiver coils [8] ADNI instituted an image nonuniformity postprocessing step for all 3D T1 scans. These produced significant improvement in uniformity for individual scans and reduction in the normalized difference image variance when using masks that identified distinct brain tissue classes, and when using smaller spline smoothing distances (e.g., 50–100 mm) for magnetization prepared rapid acquisition gradient echo sequences. These optimized settings may assist future large-scale studies where 3T scanners and multiarray receiver coils are used, such as ADNI, so that intensity nonuniformity does not influence the power of MR imaging to detect disease progression and the factors that influence it [9].

A second technical problem was image distortion due to gradient nonlinearity. The three major vendors have had different levels of distortion correction for 3D scans depending on scanner software version. Some software versions had full 3D correction, some 2D correction, and in some cases images were acquired with no distortion correction. Offline gradient distortion correction was applied as necessary by the MR core to bring all images to the equivalent of a full 3D correction for all 3D T1 images. Over time, all vendors ultimately provided 3D correction as product, consequently distortion correction in now accomplished using on-scanner vendor product methods.

The final image artifact ADNI addressed was changes in geometric scaling over time. Initially, the ADNI phantom was scanned with each patient examination and this information was used to correct for changes in scanner geometric scaling over time. However, analyses performed by the ADNI-MRI core revealed that linear scaling through image registration performed this task as well or better than correction by simultaneous phantom measurement; and scaling corrections, by either method, reduced within-subject variability and thereby sample size estimates by 10% or more [10]. Moreover, with improvements in scanner design over time, significant scaling drift became uncommon. Consequently, the use of the ADNI phantom for this purpose was discontinued in ADNI-2.

2.3. MR measures performed

The operations of the MRI core described to this point addressed technical issues of protocol design, site qualification, QC, and image postprocessing. However, a second major thrust of the core was to provide quantitative measures that were relevant to AD clinical trials. The research groups of the ADNI core responsible for providing specific measures are listed below.

Structural MRI measures: boundary shift integral—University College London (UCL); Freesurfer—San Francisco VA (SFVA); tensor-based morphometry (TBM)—University Southern California (USC); TBM-Syn—Mayo Clinic; quantitative anatomical regional change—Quarc (University of California San Diego); cerebrovascular disease—UC Davis; cerebral microbleeds—Mayo; ASL—SFVA; hippocampal subfields—SFVA; DTI—USC; TF-fMRI—Mayo.

Results from these analyses have had a wide ranging impact. Some results are listed below by topic. Topics were selected for presentation that addressed the central aim of ADNI of improving clinical trial methods, were the subject of large numbers of reports in the literature, or both.

2.4. Assessing effects of MRI hardware on structural MRI measures, and methods for accommodating these effects

When ADNI 1 began, clinical practice at many academic centers was transitioning from 1.5T scanners to 3T; however, many sites had not made this transition. Consequently, clinical trials in AD were typically being carried out at 1.5T [1]. One of the aims of ADNI 1 was to compare structural MRI

measures at 1.5T versus 3T to determine if field strength had a significant impact on quantitative measures that were relevant to AD clinical trials. ADNI investigators found that the two field strengths were roughly comparable with no major drawbacks unique to either [11,12]. Because of greater signal to noise and the greater flexibility for more advanced scanning techniques at 3T, ADNI-GO/2 was conducted entirely at 3T [3].

2.5. Use of acceleration for 3D T1 MRI

One of the questions that arose during the design phase for the ADNI-GO/2 MR protocol was should the 3D T1 sequence be accelerated? Acceleration reduces imaging time, allows more sequences to be acquired in an imaging session of fixed duration, and potentially could reduce motion-related artifacts, albeit with the penalty of reduced signal to noise compared with nonaccelerated imaging. The literature available during the planning of ADNI-GO/2 did not provide a definitive answer to this question. Therefore, ADNI-2 was designed to assess the effect of acceleration on quantitative measures used in AD clinical trials.

Analyses by the MR core did not detect consistent difference between quantitative measures from accelerated versus unaccelerated acquisitions. Two studies [13,14] applied tensor-based morphometry (TBM) to measure brain changes in accelerated and nonaccelerated MRI scans, and no significant difference was detected in numerical summaries of atrophy rates over a 6- and 12-month scan interval, in any patient group or in controls. Whole-brain, voxel-wise mapping analyses revealed some apparent regional differences in 6-month atrophy rates when comparing all subjects irrespective of diagnosis ($n = 345$), but no such whole-brain difference was detected for the 12-month scan interval ($n = 156$). Scan acceleration may influence some brain measures, but had minimal effects on TBM-derived atrophy measures, and effect sizes for structural brain changes were not detectably different in accelerated versus nonaccelerated data.

Changing from unaccelerated to accelerated scans within an individual subject's time series typically causes major problems for measurements of change over time but with postprocessing methods to compensate for contrast differences atrophy rates could be measured with relatively little adverse effect for some but very noticeable effects for other vendor systems [15]. Therefore, based on the data from ADNI-GO/2, our recommendation is that the acceleration of 3D T1 scans for morphometry is not harmful, but a given study should choose one approach or the other and use that approach consistently.

2.6. Improved image processing methods for structural MRI, and sample size estimates for clinical trial design

ADNI-MRI data have been used extensively to develop and evaluate the utility of new methods to analyze anatomic MRI data, particularly longitudinal data as a potential outcome measure in clinical trials. Methods that have been applied extensively to ADNI data include tensor-based morphometry (TBM) [16–18], free surfer, improvements to the boundary shift integral (BSI) [19], and quantitative anatomical regional change (Quarc) [20–24].

TBM, for example, was used to estimate rates of structural brain atrophy, $N = 5738$ scans, from ADNI participants scanned with both accelerated and nonaccelerated T1-weighted MRI at 3 Tesla [25]. TBM uses nonlinear image registration, sometimes based on elasticity or fluid mechanics, to "warp" or compress an individual's baseline scan onto a subsequent scan. The resulting warping field reveals the whole profile of atrophy or expansion as a color-coded map (Fig. 1), and tissue loss rates can be summarized in regions of interest, such as the hippocampus or temporal lobe. Some groups proposed the use of "statistically predefined regions of interest (ROIs)"—or stat-ROIs—that used a portion of the scan data to identify regions that change the most, or that differ the most between patients and controls. To avoid circularity, changes in these regions were computed on the rest of the data. Several papers noted that atrophy rates computed in these stat-ROIs were higher than standard anatomical regions of interest such as the temporal lobes, offering greater effect sizes to detect change and group differences. A further advance used linear discriminant analysis (LDA) to home in on regions of the image to compute atrophy. Gutman et al. [26] showed how to incorporate different features (changes in ventricular surface, Jacobians from TBM) in an LDA framework to generate a weighted map used for identifying a univariate summary measure that could be used to measure disease progression, and potentially disease modification of a successful intervention. By incorporating information from surface models of the lateral ventricles, with TBM measures, this method, which uses continuous weights on the features, performed much better than the binary hard thresholding approach of the "statistical" ROI. It also provides lower sample sizes (in some cases with potentially nonoverlapping confidence intervals) with other well-established methods.

Taking advantage of the large amount of serial MRI data generated in ADNI-1 it was possible to make improvements to the BSI (Fig. 2) to provide longitudinally consistent multi-time-point atrophy rate measurements [19]. Such consistency and lack of bias is particularly important for longer studies with multiple imaging time points which have become increasingly common in AD trials [27]. Automation of analysis methods is particularly valuable for large studies. Based on template-based and label fusion methods, accurate and fully automated brain and hippocampal segmentation algorithms were developed and validated in ADNI [28–31]. The automated and manual segmentations produced very similar results (Jaccard Index >0.98 for brain and >0.80 for hippocampus). This contributed to the European Medical Agency's decision to approve the use of hippocampal volume measures to enrich clinical trial

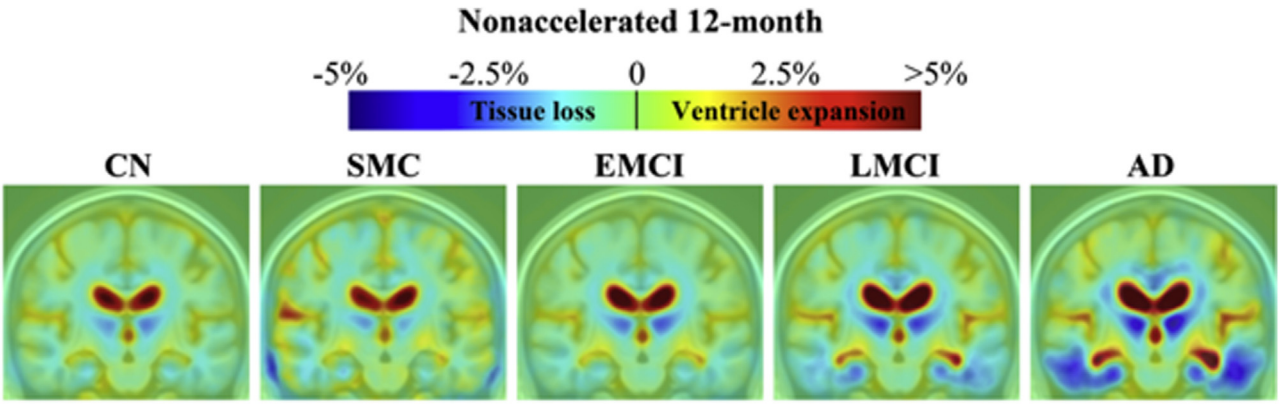

Fig. 1. Tensor-based morphometry (TBM). This figure, adapted from Hua et al. [25] shows how TBM can visualize the profiles of brain tissue loss and expansion, throughout the brain, in this case over a 12-month interval. These average maps of brain tissue loss for different diagnostic groups can be summarized to produce single "numeric summaries" of atrophy rates, as a percentage per year. Brain regions offering greatest group discrimination included the temporal lobes (shown in blue), or specially defined regions within them.

populations in prodromal AD/mild cognitive impairment (MCI). The automated segmentation was combined with the boundary shift integral to provide a fully automated image processing pipeline for accurate and consistent brain and hippocampal atrophy measurements over multiple time points; such automation, avoiding manual involvement and potential bias, was attractive for trials potentially seeking regulatory approval [32].

A common metric by which different algorithms have been assessed are sample size estimates for clinical trials. Using a therapeutically induced reduction in the natural rate of atrophy as an outcome measure could considerably reduce sample sizes needed for trials. ADNI has contributed significantly to growth in this area and rates of change on anatomic MR have consistently performed quite well in comparison to all other biomarker and cognitive indices [24,33–37].

One group applied LDA to features from TBM and surface models of ventricular regions, to identify brain regions that gave highest effect sizes in detecting brain change rates and group differences. A 2-year trial using these measures requires 31 (point estimate) AD subjects, or 56 subjects with MCI to detect 25% slowing in atrophy with 80% power and 95% confidence [26]. In a head-to-head comparison on all available ADNI-1 data, Gutman et al. [26], FreeSurfer ventricular measures give 2-year point estimates of 90 for AD and 153 for MCI. An FMRIB Software Library tool, known as SIENA, achieved a 1-year point estimate for sample size of 132 for AD and 278 for MCI. Quarc entorhinal measures achieved 2-year point estimates of 44 for AD and 134 for MCI. MRI measures commonly offered greater effect sizes than typical clinical and positron emission tomography (PET)-derived measures derived in the same subjects.

In comparing MRI metrics of brain change, some important lessons were learned. As some methods fail on some subsets of the scan data, Wyman et al. [38] advocated that all head-to-head comparisons of methods be conducted on the same data set, explicitly noting any data throw-out; this effort led to the definition of "standard" MRI data sets for ADNI. Second, some early versions of TBM

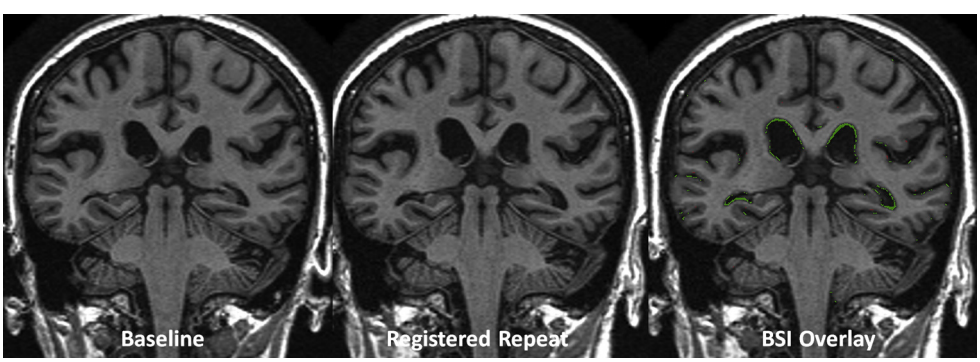

Fig. 2. Boundary shift integral (BSI). Coronal, volumetric (three-dimensional or 3D) T1-weighted MRI scans from the same individual scanned at baseline and after an interval are shown. The second scan is aligned (spatially registered) to the first. Atrophy occurring between the two scans results in a shift at the brain/cerebrospinal fluid (CSF) interface (green overlay on third image). The BSI, the sum of the displacement of the brain/CSF boundary across the whole brain, provides a means of quantifying atrophy occurring between the two scans.

overestimated brain changes due to very complex sources of bias in the method (see Hua et al., 2015 [25] for an unbiased method and a discussion). Arguably, these methodological improvements would not have been identified without the many time points collected by the ADNI-MRI data sets, which allowed consistencies and nonlinearities in the brain changes to be critically evaluated with multiple independent methods.

To guide future trial design it was important for ADNI to provide a realistic "real-world" model of phase 2/3 trial data including all the heterogeneity in scanners inevitable in large multicenter studies. ADNI included therefore multiple manufacturers, scanner types, and software versions. This meant that MR-based metrics could be needed to accommodate this heterogeneity and be tested on it. Tissue-specific intensity normalization and parameter selection was introduced to the BSI to create the K-means normalized BSI (KN-BSI); this was shown to significantly improved sample size estimates [39]. Estimated sample sizes using whole brain atrophy rate with KN-BSI were shown to be 20% lower than for the previous classic BSI. To give 80% power to detect a 25% reduction in progression while controlling for normal aging: samples sizes (95% CI) using KN-BSI were 223 subjects per arm (154, 342), compared with 284 (183, 480) for classic BSI [31]. In addition, a generalized BSI was developed by estimating adaptively a nonbinary exclusive or region of interest from probabilistic brain segmentations of the baseline and repeat scans, to better localize and capture the brain atrophy [40]; sample sizes were reduced by a further 15%. These advances, developed and tested in ADNI, have gone on to be adopted in several phase 3 trials [41].

Using the clinical and biomarker detail available in ADNI it was possible to show the MR-based sample sizes estimates could potentially be further reduced by adjusting for baseline characteristics such as disease severity or measures of amyloid pathology [37]; adjusting for 11 predefined covariates reduced sample size estimates by up to 30%.

When using the rate of atrophy as an outcome measures, it is important to recognize that not all structural changes that occur over time in older adults are attributable to latent AD pathology [42,43]. Thus it is important to take into account changes that occur in normal aging when calculating sample size estimates when atrophy is used as an outcome variable [22,24,27,44,45].

Heterogeneity among groups was also addressed. The diagnostic category of MCI contains subgroups that experiences different rates of cognitive decline [46,47]. The same is true of subjects classified as cognitively normal (CN). For example, older patients decline at a slower rate than younger patients [24,48]; in some studies women decline at a faster rate than men [49]; individuals who test positive for cerebrospinal fluid (CSF) amyloid or tau pathology decline at a faster rate than those who do not [50]; individuals who show atrophy [44,50] or a positive amyloid PET scan [51] at baseline decline faster than those who do not; individuals who carry the *APOE* ε4 allele decline at a faster rate than those who do not [44,49].

2.7. Predicting future clinical/cognitive decline

In the context of improving methods for clinical trials a question of interest has been the efficacy of various biomarkers, including MRI, in predicting future cognitive decline. Selecting subjects for inclusion in clinical trials who are likely to decline cognitively over the typically short duration of a clinical trial can reduce costs considerably [22,24,44,50,52]. A number of studies have used ADNI data to assess this and have generally found that MRI is as effective as any biomarker (or more so) in predicting short-term future clinical decline [53–57]. These studies contributed to the European Medical Agency's decision to approve the use of hippocampal volume to enrich clinical trial populations in prodromal AD/MCI [58,59].

Many MR measures beyond hippocampal volume, however, are predictive of cognitive decline. For example, temporal and parietal volumes can identify cognitively healthy individuals who are at risk for future memory decline. In particular, use of the most accurate region model, which included the hippocampus, parahippocampal gyrus, amygdala, superior, middle, and inferior temporal gyri, superior parietal lobe, and posterior cingulate gyrus, resulted in a fitted accuracy of 94% and a cross-validated accuracy of 81% [52].

Analyses using Freesurfer software [60] demonstrated that enforcing local linearity on the imaging features using an unsupervised learning algorithm called local linear embedding [61] were able to better train classifiers, such as support vector machines for predicting future conversion to AD from baseline MRI scans [62]. Most strikingly, the approach significantly improved predictions whether MCI subjects remained stable within a 3-year period or converted to AD. In another study [63] atrophy rates in some brain regions, including the hippocampus and entorhinal cortex, generally varied nonlinearly with age and furthermore leveled off with increasing age in normal and stable MCI subjects in contrast to MCI converters and AD patients, whose rates progressed further.

2.8. Associations between structural MRI and cognitive performance, CSF biomarkers, and PET

Numerous studies have been performed with ADNI data assessing associations between structural MRI and cognitive performance, CSF biomarkers, or PET. Results and conclusions from these studies are too extensive to catalog here but some representative findings are outlined later.

One of the goals of ADNI was to compare the ability of different biomarkers to distinguish cross-sectionally between different patient groups. All biomarkers (MRI, fluorodeoxyglucose positron emission tomography, and CSF) can distinguish between diagnostic groups of healthy controls,

MCI, and mild AD patients [64]. However, these measures are complementary, and the combined use of different types of biomarkers can improve the diagnostic discrimination and prediction of decline [53,65–69]. CSF amyloid beta (Aβ) and florbetapir PET were independent predictors of several AD features, including brain structure, brain function, CSF tau, and cognitive impairment. Isolated low CSF Aβ with normal florbetapir PET was most common in healthy controls, and least common in AD dementia. The findings suggest that CSF Aβ and florbetapir PET partly capture different aspects of amyloid pathology and that these may differ by disease stage [70].

Examining the association of different biomarkers with rates of change in structural MRI can provide insight into the pathobiological basis of the disease. For example, amyloid pathology, as evidence by low CSF Aβ levels, was associated with clinical decline and accelerated neurodegeneration only in the presence of elevated CSF phosphorylated tau [71,72]. Other proteins, such as heart fatty acid binding protein and clusterin may also be implicated in AD neurodegeneration, as they were associated with increased atrophy in medial temporal lobe among individuals with low CSF Aβ, irrespective of CSF phospho-tau181p status [73,74].

Aβ pathology, estimated by CSF Aβ, is associated with atrophy already before reaching previously established cutoffs for abnormality [75]. Supporting this view, CSF Aβ in the low normal range was associated with the development of CSF Aβ positivity within 3 years, suggesting emerging amyloid pathology [76]. Furthermore, longitudinal reductions in CSF Aβ (from normal baseline levels) were associated with accelerated atrophy in CN controls, suggesting early effects of amyloid pathology on brain structure [77].

Baseline CSF Aβ predicts the progression of hippocampal volume loss across the clinical groups in the AD continuum. *APOE* ε4 carrier status amplifies the degree of neurodegeneration in MCI. Understanding the effect of interactions between genetic risk and amyloid pathology will be important in clinical trials and our understanding of the disease process [78].

In CN older adults and subjects with MCI, age and Aβ have independent effects on hippocampal atrophy rate. In a multivariable model including age, Aβ, *APOE* ε4 genotype, gender, and white matter lesions, only Aβ status is significantly associated with hippocampal atrophy rate. Hippocampal atrophy rate is higher in Aβ+ participants, but most hippocampal atrophy rate is not accounted for by Aβ status in either cohort. Because treatments directed at reducing Aβ would not be expected to slow the non-Aβ-related hippocampal atrophy rate, these results can inform the design of future clinical trials testing the efficacy of such therapies in CN and MCI individuals [79].

Lower CSF Aβ and higher tau concentrations were associated with increased rates of regional brain tissue loss [80] and the patterns varied across the clinical groups. CSF biomarker concentrations are associated with the characteristic patterns of structural brain changes in CN and MCI that resemble to a large extent the pathology seen in AD. Therefore, the finding of faster progression of brain atrophy in the presence of lower Aβ levels and higher p-tau levels supports the hypothesis that CSF Aβ and tau are measures of early AD pathology. Moreover, the relationship among CSF biomarkers, *APOE* ε4 status, and brain atrophy rates are regionally varying, supporting the view that the genetic predisposition of the brain to amyloid and tau mediated pathology is regional and disease stage specific [81,82].

Regional brain atrophy and metabolism partly mediate the effects of CSF Aβ on longitudinal cognition in MCI. The mediating effects of atrophy and metabolism were additive, explaining up to ∼40% of the effects of CSF Aβ. However, CSF Aβ also had effects on cognition that were not captured by these changes in brain structure and function, and brain structure/function was also related to cognition independently of amyloid [83]. Low cerebral perfusion is associated with CSF Aβ pathology in normal, MCI, and AD [84].

In MCI, increased Aβ burden in the left precuneus/cuneus and medial-temporal regions was associated with increased brain atrophy rates in the left medial-temporal and parietal regions; and in contrast, increased Aβ burden in bilateral precuneus/cuneus and parietal regions was associated with increased brain atrophy rates in the right medial temporal regions. The results could be used to develop a specific AD-specific imaging signature for diagnosis [85]. ADNI results from a different analysis, however, do not support the notion of a consistent AD-specific signature of atrophy based on comparing amyloid PET positive versus negative CN elderly [86].

In an attempt to identify a neuroimaging signature predictive of brain amyloidosis as a screening tool to identify individuals with MCI that are most likely to have high levels of brain amyloidosis or to be amyloid free, it was shown that Aβ positivity in late MCI could be predicted with an 88% accuracy (with >90% sensitivity and specificity at 20% false-positive rate and false-negative rate thresholds) using a structural MRI-based brain amyloidosis signature and *APOE* genotype. The performance of hippocampal volume as an independent predictor of brain amyloidosis in MCI was only marginally better than random chance (56% classification accuracy). Aβ-positive early MCIs could be identified with 83% classification accuracy, 87% positive predictive value, and 84% negative predictive value by multidisciplinary classifiers combining demographics data, *APOE* ε4-genotype, and a multimodal MRI-based Aβ score combining structural and perfusion signatures of brain amyloidosis [87,88].

A network diffusion model to mathematically predict disease topography resulting from the transneuronal transmission of neurodegeneration on the brain's connectivity network was used to predict the future patterns of regional atrophy and metabolism from baseline regional patterns of atrophy. The model accurately predicts end-of-study regional atrophy and metabolism starting from baseline

data, with significantly higher correlation strength than given by the baseline statistics directly. The model's rate parameter encapsulates overall atrophy progression rate; group analysis revealed this rate to depend on diagnosis and baseline CSF biomarker levels. This work helps validate the model as a prognostic tool for AD assessment [89].

Among individuals with MCI, those with subsyndromal symptoms of depression had a lower volume of white matter lesions and a higher frequency of *APOE* ε4 alleles than individuals without symptoms of depression. At baseline, subsyndromal symptoms of depression individuals showed significantly more disability than individuals with no symptoms of depression after controlling for the effect of cognitive functioning, intracranial brain volume, white matter lesions, and *APOE* status [90].

Many ADNI reports have attempted to determine which CSF and cognitive measures, and which blood biomarkers are most highly correlated with brain atrophy on MRI, and which changes in imaging and other biomarkers were most tightly linked. Although the core pathology of AD is clearly linked with changes on MRI [91,92], several papers identified and explored associations between atrophy on MRI and body mass index, measures of physical exercise, diabetes, homocysteine levels [93], and a range of hormone measures (e.g., leptin [94]), lipid, and metabolic markers obtainable from standard blood tests. Some groups advocated measuring these markers in any MRI-based clinical trial, as they may offer added value in predicting atrophy or brain reserve beyond tests of classical AD pathology in the brain or CSF [95].

2.9. Modeling biomarker trajectories

One of the objectives of ADNI-2 was to assess the temporal evolution of the different AD biomarkers outlined in a hypothetical biomarker model published in 2010 [96,97]. The hypothesis to be tested was that biomarkers of brain amyloidosis became abnormal in the preclinical phase of the disease, but their rate of change plateaus [98,99] as overt clinical symptoms evolve such that the correlation between amyloid biomarkers and clinical symptoms is limited. In contrast, biomarkers of neurodegeneration become abnormal later in the disease, but their temporal evolution correlates well with the evolution of clinical symptoms.

Several studies have examined the question of temporal ordering of AD biomarker abnormalities in autosomal dominant AD [100–103]. These have uniformly supported the proposed sequence of events proposed in the hypothetical model [96,97,104] where biomarkers of b-amyloidosis become abnormal first, followed by tau or FDG (depending on the study), followed by structural MRI, followed lastly by overt clinical symptoms.

Studies in elderly subjects address sporadic AD and ADNI studies fall into this category. Studies using data from ADNI or other elderly cohorts to test this biomarker model (with one exception [105]) have shown that empiric data [98,99,106–111] largely supports the principles outlined hypothetically [96,97]. The difficulty in studying AD biomarkers in elderly subjects is that older subjects with AD typically have AD mixed with other age-related non-AD pathologies. Thus attributing cognitive or neurodegenerative biomarker abnormalities exclusively to AD is confounded by the fact that both cognition and neurodegeneration occur due to co-occurring non-AD features of aging. The problems that SNAP (suspected non-Alzheimer's pathophysiology) [104,112] presents in modeling AD biomarkers in elderly subjects are discussed in the following paragraph.

An event-based model was developed to make use of the multimodal data sets available in ADNI [106]. This allowed the determination of the sequence in which AD biomarkers become abnormal without reliance on a priori diagnostic information or explicit biomarker cut points. This data-driven model supported the hypothetical model [96,97] of biomarker ordering in amyloid-positive and *APOE*-positive subjects, but suggested that biomarker ordering in noncarriers might diverge from this sequence. However, apparent divergence from the hypothetical model [96,97] in *APOE* noncarriers is very likely due to the fact that AD-like neurodegenerative biomarker abnormalities (anatomic MRI, FDG PET, and CSF tau) in amyloid *negative* individuals becomes a progressively more prevalent condition in the population with advancing age [113]. This condition, neurodegeneration positive but amyloid negative, has been termed suspected nonamyloid pathophysiology (or SNAP) [114]. The onset of amyloidosis in the population is accelerated by roughly 7 years in *APOE* carriers relative to noncarriers [115]. Thus modeling of AD biomarker ordering is particularly difficult in elderly *APOE* noncarriers due to the high prevalence of SNAP in the elderly. Individuals without amyloidosis are increasingly more likely to have non-AD aging-related neurodegeneration (i.e. SNAP) with advancing age [112].

2.10. Use of structural MRI in the assessment of new diagnostic criteria for AD in its different clinical phases (preclinical, MCI/prodromal, and AD dementia)

Two major working groups have published updated diagnostic criteria for AD in recent years [116–120]. These modern criteria use imaging and CSF biomarkers to improve diagnostic certainty and disease specificity. Structural MRI is one of the imaging measures used in all diagnostic criteria in all clinical phases (preclinical, MCI/prodromal, and AD dementia). Several groups have used the ADNI data to assess validity and utility of these new diagnostic criteria [114,121–130].

2.11. Associations between MR and genetic variants

A number of studies have assessed the effect of *APOE* ε4 on structural MRI both cross-sectionally and longitudinally. *APOE* ε4 has consistently been found to be associated with

higher rates of atrophy across all clinical stages of the disease—including CN subjects. In particular hippocampal atrophy rates in ε4 carriers were shown to be higher in AD and MCI subjects compared with *APOE* ε4 noncarriers [131]. Even after adjustment for whole-brain atrophy rate, the difference in hippocampal atrophy rate between ε4 carriers and noncarriers remained statistically significant in AD and (only) in those MCI subjects who progressed to AD.

A further innovation was the use of genome-wide screening in conjunction with ADNI-MRI data to identify common genetic variants that might predict brain changes [132,133]; these are reported as part of the ADNI Genetics Core paper (this issue). Notably, some studies related brain atrophy on MRI to variants in candidate genes such as the obesity-associated gene, *FTO* [134], dopamine-related genes [135], opiate receptor genes [136], folate-related genes [137], and rare variants that confer high odds ratio of AD, such as *TREM2* [138]. Confirmation of these genetic effects requires very large samples, and ADNI has contributed to several high-profile papers analyzing brain MRI in over 30,000 individuals [139].

2.12. Use of ADNI scans to create a harmonized definition of the hippocampus

Perhaps the most common anatomic structure measured on structural MRI in the AD field is the hippocampus. However, boundary definitions vary widely from center to center. Accordingly, one of the needs in the field identified several years ago was a standardized definition of hippocampal boundaries [140]. A consortium led by Giovanni Frisoni has successfully addressed this issue [141–143]. ADNI was the source of MRI data for the hippocampal harmonization effort.

2.13. Impact of cerebrovascular disease

Coincident vascular brain injury is a common feature of individuals diagnosed with dementia, including dementia attributed to AD [144]. Therefore, despite the focus of ADNI to study the effects of AD on diagnosis and prognosis, the evaluation of vascular brain injury in ADNI is very relevant to understanding the specific effects of AD pathology on cognition to guide potential inclusion or stratification strategies in future AD trials. Initial work developed an automated method to detect white matter hyperintensities (WMH) [145]. Follow-up work in 804 subjects [146] found that the extent of baseline and change in WMH volume was associated with cognitive decline. Moreover, despite the low level of vascular risk factors in the subject cohort, a significant association between the extent of vascular risk and extent of WMH was found. Follow-up studies found that both the extent of WMH volume and levels of CSF Aβ and tau were associated with an increased rate of cerebral atrophy [147] and showed that both WMH and CSF amyloid levels influence cerebral glucose metabolism and contributed to risk for conversion from MCI to dementia in ADNI [148]. These publications strongly suggest that vascular risk factors and WMH have a significant impact on brain structure, function, and cognition within even a well-selected clinical study population as modeled by ADNI suggesting that subtle vascular risk and WMH—which have effects independent of biomarkers of AD—should be taken into account when designing clinical trials [149].

Comorbid disease processes, particularly the influence of vascular disease, would be expected to be a common confounding effect [150] when attempting to identify the earliest cognitive changes associated with AD pathology. Biological heterogeneity is a consequence of mixed pathological causes of cognitive impairment among individuals diagnosed with presumed AD pathology. A series of publications by Nettiksimmons et al. examine this issue [151–153]. Initial analyses [153] used an unsupervised clustering method using 11 different biomarkers identified three separate subtypes within the CN cohort of ADNI. Comparison of biomarkers found that group 3 had biomarker measures that were similar to MCI and AD patients and showed significant worsening of cognition over time, whereas group 1 looked most normal on these measures, whereas group 2 had MRI measures consistent with MCI and AD patients, but lacked CSF amyloid indices of AD suggesting that this group was similar to the recently identified SNAP [114]. Follow-up analysis of group 2 by Nettiksimmons et al. [151] found that these individuals had increased prevalence of vascular risk factors, WMH, and atrophy supporting the notion that vascular brain injury is common to a CN elderly cohort. Nettiksimmons et al. subsequently extended heterogeneity analysis to the MCI cohort [152]. In this case, despite the assumption that the amnestic MCI is a strong AD phenotype [154], four separate groupings were identified. Similar to the previous studies, group 1 was normal on all biological markers. Groups 2 and 3, however, appeared to have varying degrees of AD pathological signature, with group 2 having normal appearing brain structural measures. Group 4, which was the smallest, had a biological marker signature identical to AD. The authors concluded by emphasizing the biological heterogeneity despite nearly identical clinical phenotype and again emphasized the need to assess this biological heterogeneity when considering future treatment trials.

Estimates of premorbid intelligence quotient (possible cognitive reserve) and biomarkers of neuronal damage, including WMH, and amyloid pathology were shown to be independent determinants of cognition [155].

Overall, measures of vascular disease in ADNI show that concomitant WMH additive contributes to brain injury and rate of cognitive decline which increases biological heterogeneity and may influence response to treatments specifically targeting AD pathology. Future studies using the expanded clinical phenotypes of ADNI-2 are likely to add to the understanding of the influence of even mild vascular brain injury on aging cognitive trajectories.

2.14. Cerebral microbleeds

A T2* gradient echo scan was added to ADNI-GO/2 to acquire detailed information about CMB and superficial sidersosis. This was prompted by findings of increased risk incident CMBs in individuals receiving immunotherapy for AD and concerns raised about the risk this posed for patients with CMBs detected at baseline [156,157]. In the ADNI cohort, the prevalence of superficial siderosis at baseline was 1% and the prevalence of CMB was 25% [158]. The baseline prevalence of CMB increased with age and β-amyloid load. *APOE* ε4 carriers had higher numbers of CMB compared with *APOE* ε3 homozygotes, however, after accounting for differences in Aβ load, the apparent ε4 effect was reduced, suggesting that the risk of CMB for *APOE* ε4 carriers is mediated by Aβ load. The topographic densities of CMBs were highest in the occipital lobes and lowest in the deep/infratentorial regions. Greater number of CMBs at baseline was associated with a greater rate of incident CMBs.

2.15. Arterial spin labeling

Arterial spin labeling (ASL) was performed on Siemens systems in ADNI-GO/2, using a pulsed labeling approach. Using an integrated multimodality MRI framework, the UCSF group studied the extent to which cortical thinning and reduced regional cerebral blood flow (rCBF) explain individually or together variability in dementia severity [159,160]. This study showed that cortical thinning dominated the classification of AD and controls compared with contributions from rCBF. However, there was also a positive interaction between reduced rCBF and cortical thinning in the right superior temporal sulcus, implying that structural and physiological brain alterations in AD can be complementary. In another ASL study, the UCSF group explored the relationship between rCBF variations and amyloid-β pathology [84]. Furthermore, the UCSF group explored whether amyloid-β has different associations with rCBF and gray matter volume. We found that a higher amyloid-β load was related to lower rCBF in several regions, independent of diagnostic group. Moreover, the associations of amyloid-β with rCBF flow and volume differed across the disease spectrum, with high amyloid-β being associated with greater cerebral blood flow reduction in controls and greater volume reduction in late MCI and dementia, potentially indicating abnormal rCBF precedes brain tissue loss.

2.16. Diffusion tensor imaging

DTI was performed on GE systems in ADNI-GO/2. A goal of ADNI-2 has been to determine the added value of diffusion-weighted MRI for understanding and monitoring brain changes in aging, MCI, and AD.

Demirhan et al. [161] quantified the added value of DTI measures, over and above structural MRI, and showed that they provided added diagnostic accuracy for the classification of disease stages. In an effort to rank which DTI-based measures were most beneficial for diagnostic classification, Nir et al. [162] found that both voxel-based maps and region-of-interest analyses revealed widespread group differences in fractional anisotropy (FA) and in all standard diffusivity measures. All DTI measures were strongly correlated with all widely-used clinical ratings (Mini Mental State Exam, Clinical Dementia Rating – sum of boxes, and Alzheimer's disease Assessment Scale – cognitive subscale). When effect sizes were ranked, *mean diffusivity* measures tended to outperform FA measures for detecting group differences. ROIs showing strongest group differentiation (greatest effect sizes) included tracts that pass through the temporal lobes, as expected, but also tracts in some posterior brain regions. The left hippocampal component of the cingulum showed consistently high effect sizes for distinguishing diagnostic groups, across all diffusivity and anisotropy measures, and in correlations with cognitive scores.

Several studies also used the ADNI-DTI scans to compute measures of anatomical connectivity, including measures of the brain's network properties. In a longitudinal study using both diffusion weighted imaging and anatomic MRI, Nir et al. [163] found that baseline DTI network measures predicted future volumetric brain atrophy in people with MCI, suggesting that DWI-based network measures may be an additional predictor of AD progression. Further work used fiber tracking (tractography) to assess the integrity of the brain's major fiber bundles. Nir et al. [164] found significant differences in mean diffusivity (MD) and fractional anisotropy between AD patients and controls, and MD differences between people with late MCI [47] and matched elderly controls. MD and FA measures from selected tracts were also associated with widely used clinical scores.

Prasad et al. [165] performed a ranking of connectivity measures, to see which ones best distinguished AD from normal aging. Graph-based network measures—such as small-world properties, clustering, and modularity—offered additional value in differentiating diagnostic subgroups relative to just using the raw connectivity matrices; there was also additional predictive value in computing a very dense connectivity matrix to represent the anatomical connectivity between all adjacent voxels in the image [166]. This approach, known as "flow-based connectivity analysis" complemented the more standard analysis of large-scale tracts interconnecting cortical and subcortical regions of interest.

Additional work assessed what kinds of methods were best for detecting diagnostically relevant features in DTI. Care is needed in clinical analyses of brain connectivity, as the density of extracted fibers, and the imaging protocol, may affect how well a network measure can pick up differences between patients and controls. Prasad et al. [167] focused on global efficiency, transitivity, path length, mean degree, density, modularity, small world, and assortativity measures computed from weighted and binary undirected connectivity matrices. Of all these measures, the mean nodal

degree—a measure of the total number of detectable connections for each brain region—best distinguished diagnostic groups. High-density fiber matrices, computed with advanced probabilistic tractography methods, were most helpful for picking up the more subtle clinical differences, for example, between MCI and normals, or for distinguishing subtypes of MCI (early versus late) [47]. Generalized low-rank approximations—a technique for filtering brain networks—and a method called "high-order singular value decomposition" both boosted disease classification accuracy based on structural brain networks [168,169].

Advanced mathematical work also identified new DTI-based metrics that showed differences between AD and healthy aging. These included analysis of the "rich club" coefficient, and a measure of the complexity of the structural backbone of the white matter, called the *k*-core [170–172]. Additional studies evaluated new measures of algebraic connectivity and spectral graph theory, and showed how they revealed new aspects of network breakdown in AD and MCI [168,173]. Additional work studied the effects of scanner upgrades on DTI measures, and ranked DTI measures in terms of their stability under upgrades in scanning protocols [174,175].

The ADNI-DTI data set also served as a public platform to develop and test new analysis methods. Jin et al. (2015), for example, used the data set to develop an algorithm for extracting the fornix from brain DTI scans—a key tract of interest when studying hippocampal fiber connections with the rest of the brain. Others studied the diffusion signal at each voxel, and found it useful as a basis for classification of AD [176].

The ADNI-DTI data were also the target of new kinds of genetic analysis. Warstadt et al. [177] found evidence that cholesterol-related genes affected white matter fiber integrity; Jahanshad et al. [178,179] used the ADNI-DTI and Genome Wide Association Study data as part of a large-scale genetic study, by the Evidence-based Network for the Interpretation of Germline Mutant Alleles consortium, to discover common genetic variants that affect brain connectivity.

2.17. Task free fMRI

Resting or task-free fMRI was performed on Philips systems in ADNI-GO/2. Major ADNI findings to date are consistent with the literature in this area. The default mode network has distinct subsystems with characteristic cognitive associations [180]. Measures of functional connectivity in the posterior default mode network decline with advancing cognitive impairment. Measures of functional connectivity in the anterior default mode network are elevated early in the disease process—that is, in amyloid positive CN individuals—but decline in later stages of dementia. These nonmonotonic associations between functional connectivity and clinical progression present challenges for the use of TF-fMRI as a simple AD biomarker, but also present opportunities for a deeper understanding of AD biology and how TF-fMRI could be used in clinical trials.

2.18. Hippocampal subfields

A high-resolution coronal acquisition for hippocampal subfield measures was performed on Siemens systems in ADNI GO/2. The ADNI 2 subfield add-on project aimed to (1) test the feasibility of acquiring high-resolution hippocampal images of high quality in a large multisite project; and (2) compare different methods for automated subfield volumetry using a standardized data set. The preliminary results suggest possible superiority of a high-resolution based automated subfield volumetry over standard T1-based hippocampal volumetry for the distinction among AD, MCI, and healthy controls [4].

3. ADNI 3 MRI

The primary objectives of ADNI-1 and -2 were to improve methods for AD clinical trials and to provide an evidence base and data sets to guide future trial designs. The objectives of the MRI core in ADNI-3 will continue this focus, but with new aims that incorporate experience gained in ADNI-2 plus technical advances in MRI. In ADNI-3 we will continue to acquire structural MRI, FLAIR, and T2*gradient recalled echo scans. Due to its high measurement precision, structural MRI continues to provide the best (smallest) sample size estimates for powering clinical trials of any measure (clinical, imaging, or biofluid). And, methods for acquisition, image processing, and analysis of structural MRI continue to advance, yielding continually improving results. Similarly, knowledge about cerebrovascular disease and microbleeds is needed in every subject in clinical trials. As a vehicle for improving clinical trials, ADNI would be incomplete without these measures.

To date results from the experimental sequences have provided information not available on structural MRI, but overall have not shown better diagnostic power compared with structural MRI. We believe that this may be due to the fact that "lowest common denominator" acquisition schemes were used to optimize homogeneity across the different MR systems within each vendor product line. Our approach in ADNI-3 will be different in that we will optimize the capabilities of the high performance systems available to ADNI. This requires that we take a two-tiered approach where more basic TF-fMRI and diffusion sequences are acquired on the lower performance systems while the most advanced possible acquisition protocols are used on high performance systems. At this point the diagnostic value of coronal high-resolution T2 for hippocampal subfield analysis is still being evaluated as a potential addition to the above.

Given that the primary objective of ADNI is to improve methods for clinical trials, it might at first seem out of scope to pursue advanced methods as described previously which cannot be performed at all sites. However, technical advances in MR are continuous. Methods that are advanced at the beginning of ADNI-3 (late 2016) are likely to be standard and widely available later in the ADNI-3 grant cycle.

Our objective is to anticipate the cycle of technical advances so that we have data demonstrating the use of advanced methods for clinical trials (or lack thereof) toward end of the ADNI-3 grant cycle when these methods should be widely available. Viewed from this perspective, incorporating methods that are considered advanced at the beginning of the ADNI-3 grant cycle fulfills the mandate of ADNI to serve the interests of AD clinical trials.

Our aims will include: creating standardized summary numeric measures for each MR modality; comparing structural MRI with PET (amyloid PET and tau PET), clinical and biofluid measures; developing or using analysis methods for high performance acquisitions that take advantage of advanced MRI technology; comparing ASL, TF-fMRI, and diffusion; comparing basic versus advanced metrics for diffusion, resting fMRI, and ASL. It is widely assumed that more advanced methods are diagnostically superior to standard measures, but this has not been formally tested in an ADNI-like environment. The design of ADNI-3 will ensure that all participants are scanned using all sequences, unlike ADNI-2, fostering the creation of standard data sets to compare what each sequence offers and fostering multimodal approaches.

RESEARCH IN CONTEXT

1. Systematic review: The authors searched PubMed for: ADNI and MRI, ADNI and DTI, ADNI and ASL, ADNI, and functional MRI. The authors' publication lists were also used in compiling the bibliography.
2. Interpretation: This article reviews contributions of the magnetic resonance imaging (MRI) core of Alzheimer's Disease Neuroimaging (ADNI) over the past decade. The major objective of the ADNI MRI core is to improve methods for clinical trials in Alzheimer's disease (AD) and related disorders. The MR core has addressed this charge at a variety of levels.
3. Future directions: The MR core is currently in planning stages for ADNI-3. If funded, ADNI-3 will continue to provide anatomic MRI, vascular MR imaging, and imaging for cerebral microbleeds. ADNI-3 will expand efforts in diffusion, perfusion, and functional connectivity MRI.

References

[1] Jack CR Jr, Bernstein MA, Fox NC, Thompson P, Alexander G, Harvey D, et al. The Alzheimer's Disease Neuroimaging Initiative (ADNI): MRI methods. J Magn Reson Imaging 2008;27:685–91.

[2] Rydberg JN, Riederer SJ, Rydberg CH, Jack CR. Contrast optimization of fluid-attenuated inversion recovery (FLAIR) imaging. Magn Reson Med 1995;34:868–77.

[3] Jack CR Jr, Bernstein MA, Borowski BJ, Gunter JL, Fox NC, Thompson PM, et al. Update on the magnetic resonance imaging core of the Alzheimer's disease neuroimaging initiative. Alzheimers Dement 2010;6:212–20.

[4] Mueller S, Yushkevich P, Wang L, Van Leemput K, Mezher A, Iglesias JE, et al. Collaboration for a systematic comparison of different techniques to measure subfield volumes: announcement and first results. Alzheimers Dement 2013;9:P51.

[5] Gunter JL, Bernstein MA, Borowski BJ, Ward CP, Britson PJ, Felmlee JP, et al. Measurement of MRI scanner performance with the ADNI phantom. Med Phys 2009;36:2193–205.

[6] Simmons A, Westman E, Muehlboeck S, Mecocci P, Vellas B, Tsolaki M, et al. The AddNeuroMed framework for multi-centre MRI assessment of Alzheimer's disease: experience from the first 24 months. Int J Geriatr Psychiatry 2011;26:75–82.

[7] ISMRM 20th Annual Meeting and Exhibition: May 5-11, 2012; Melbourne, Australia; 2012: 2456.

[8] Senjem ML, Gunter JL, Shiung MM, Petersen RC, Jack CR Jr. Comparison of different methodological implementations of voxel-based morphometry in neurodegenerative disease. Neuroimage 2005; 26:600–8.

[9] Boyes RG, Gunter JL, Frost C, Janke AL, Yeatman T, Hill DL, et al. Intensity non-uniformity correction using N3 on 3-T scanners with multichannel phased array coils. Neuroimage 2008;39:1752–62.

[10] Clarkson MJ, Ourselin S, Nielsen C, Leung KK, Barnes J, Whitwell JL, et al. Comparison of phantom and registration scaling corrections using the ADNI cohort. Neuroimage 2009;47:1506–13.

[11] Ho AJ, Hua X, Lee S, Leow AD, Yanovsky I, Gutman B, et al. Comparing 3 T and 1.5 T MRI for tracking Alzheimer's disease progression with tensor-based morphometry. Hum Brain Mapp 2010; 31:499–514.

[12] Macdonald KE, Leung KK, Bartlett JW, Blair M, Malone IB, Barnes J, et al. Automated template-based hippocampal segmentations from MRI: the effects of 1.5T or 3T field strength on accuracy. Neuroinformatics 2014;12:405–12.

[13] Ching CR, Hua X, Hibar DP, Ward CP, Gunter JL, Bernstein MA, et al. Does MRI scan acceleration affect power to track brain change? Neurobiol Aging 2015;36(Suppl 1):S167–77.

[14] The 15th International Conference on Medical Image Computing and Computer Assisted Intervention (MICCAI): 2012; Nice, France; 2012.

[15] Leung KK, Malone IM, Ourselin S, Gunter JL, Bernstein MA, Thompson PM, et al. Effects of changing from non-accelerated to accelerated MRI for follow-up in brain atrophy measurement. Neuroimage 2015;107:46–53.

[16] Hua X, Gutman B, Boyle C, Rajagopalan P, Leow AD, Yanovsky I, et al. Accurate measurement of brain changes in longitudinal MRI scans using tensor-based morphometry. Neuroimage 2011;57:5–14.

[17] Leow AD, Yanovsky I, Parikshak N, Hua X, Lee S, Toga AW, et al. Alzheimer's disease neuroimaging initiative: a one-year follow up study using tensor-based morphometry correlating degenerative rates, biomarkers and cognition. Neuroimage 2009;45:645–55.

[18] Morra JH, Tu Z, Apostolova LG, Green AE, Avedissian C, Madsen SK, et al. Automated 3D mapping of hippocampal atrophy and its clinical correlates in 400 subjects with Alzheimer's disease, mild cognitive impairment, and elderly controls. Hum Brain Mapp 2009;30:2766–88.

[19] Leung KK, Ridgway GR, Ourselin S, Fox NC. Consistent multi-time-point brain atrophy estimation from the boundary shift integral. Neuroimage 2012;59:3995–4005.

[20] Fjell AM, Walhovd KB, Fennema-Notestine C, McEvoy LK, Hagler DJ, Holland D, et al. One-year brain atrophy evident in healthy aging. J Neurosci 2009;29:15223–31.

[21] McDonald CR, McEvoy LK, Gharapetian L, Fennema-Notestine C, Hagler DJ Jr, Holland D, et al. Regional rates of neocortical atrophy from normal aging to early Alzheimer disease. Neurology 2009; 73:457–65.
[22] Holland D, Brewer JB, Hagler DJ, Fenema-Notestine C, Dale AM, Weiner M, et al. Subregional neuroanatomical change as a biomarker for Alzheimer's disease. Proc Natl Acad Sci U S A 2009; 106:20954–9.
[23] Holland D, Dale AM. Nonlinear registration of longitudinal images and measurement of change in regions of interest. Med Image Anal 2011;15:489–97.
[24] Holland D, Desikan RS, Dale AM, McEvoy LK. Rates of decline in Alzheimer disease decrease with age. PLoS One 2012;7:e42325.
[25] Hua X, Ching CR, Mezher A, Gutman B, Hibar DP, Bhatt P et al. MRI-based brain atrophy rates in ADNI Phase 2: acceleration and enrichment considerations for clinical trials. Submitted to Neuroimage 2015.
[26] Gutman BA, Wang Y, Yanovsky I, Hua X, Toga AW, Jack CR Jr, et al. Empowering imaging biomarkers of Alzheimer's disease. Neurobiol Aging 2015;36(Suppl 1):S69–80.
[27] Fox NC, Ridgway GR, Schott JM. Algorithms, atrophy and Alzheimer's disease: cautionary tales for clinical trials. Neuroimage 2011;57:15–8.
[28] Hoang Duc AK, Modat M, Leung KK, Cardoso MJ, Barnes J, Kadir T, et al. Using manifold learning for atlas selection in multi-atlas segmentation. PLoS One 2013;8:e70059.
[29] Jorge Cardoso M, Leung K, Modat M, Keihaninejad S, Cash D, Barnes J, et al. STEPS: Similarity and Truth Estimation for Propagated Segmentations and its application to hippocampal segmentation and brain parcelation. Med Image Anal 2013;17:671–84.
[30] Leung KK, Barnes J, Modat M, Ridgway GR, Bartlett JW, Fox NC, et al. Brain MAPS: an automated, accurate and robust brain extraction technique using a template library. Neuroimage 2011; 55:1091–108.
[31] Leung KK, Barnes J, Ridgway GR, Bartlett JW, Clarkson MJ, Macdonald K, et al. Automated cross-sectional and longitudinal hippocampal volume measurement in mild cognitive impairment and Alzheimer's disease. Neuroimage 2010;51:1345–59.
[32] Leung KK, Bartlett JW, Barnes J, Manning EN, Ourselin S, Fox NC. Cerebral atrophy in mild cognitive impairment and Alzheimer disease: rates and acceleration. Neurology 2013;80:648–54.
[33] Hua X, Hibar DP, Ching CR, Boyle CP, Rajagopalan P, Gutman BA, et al. Unbiased tensor-based morphometry: improved robustness and sample size estimates for Alzheimer's disease clinical trials. Neuroimage 2013;66:648–61.
[34] Grill JD, Di L, Lu PH, Lee C, Ringman J, Apostolova LG, et al. Estimating sample sizes for predementia Alzheimer's trials based on the Alzheimer's Disease Neuroimaging Initiative. Neurobiol Aging 2013;34:62–72.
[35] Gutman BA, Hua X, Rajagopalan P, Chou YY, Wang Y, Yanovsky I, et al. Maximizing power to track Alzheimer's disease and MCI progression by LDA-based weighting of longitudinal ventricular surface features. Neuroimage 2013;70:386–401.
[36] Kohannim O, Hua X, Hibar DP, Lee S, Chou YY, Toga AW, et al. Boosting power for clinical trials using classifiers based on multiple biomarkers. Neurobiol Aging 2010;31:1429–42.
[37] Schott JM, Bartlett JW, Barnes J, Leung KK, Ourselin S, Fox NC. Reduced sample sizes for atrophy outcomes in Alzheimer's disease trials: baseline adjustment. Neurobiol Aging 2010;31(8):1452–62. 1462.e1–2.
[38] Wyman BT, Harvey DJ, Crawford K, Bernstein MA, Carmichael O, Cole PE, et al. Standardization of analysis sets for reporting results from ADNI MRI data. Alzheimers Dement 2013;9:332–7.
[39] Leung KK, Clarkson MJ, Bartlett JW, Clegg S, Jack CR Jr, Weiner MW, et al. Robust atrophy rate measurement in Alzheimer's disease using multi-site serial MRI: Tissue-specific intensity normalization and parameter selection. Neuroimage 2010;50:516–23.
[40] Prados F, Cardoso MJ, Leung KK, Cash DM, Modat M, Fox NC, et al. Measuring brain atrophy with a generalized formulation of the boundary shift integral. Neurobiol Aging 2015;36(Suppl 1):S81–90.
[41] Salloway S, Sperling R, Fox NC, Blennow K, Klunk W, Raskind M, et al. Two phase 3 trials of bapineuzumab in mild-to-moderate Alzheimer's disease. N Engl J Med 2014;370:322–33.
[42] Fjell AM, McEvoy L, Holland D, Dale AM, Walhovd KB. Brain changes in older adults at very low risk for Alzheimer's disease. J Neurosci 2013;33:8237–42.
[43] Fjell AM, McEvoy L, Holland D, Dale AM, Walhovd KB. What is normal in normal aging? Effects of aging, amyloid and Alzheimer's disease on the cerebral cortex and the hippocampus. Prog Neurobiol 2014;117:20–40.
[44] McEvoy LK, Edland SD, Holland D, Hagler DJ Jr, Roddey JC, Fennema-Notestine C, et al. Neuroimaging enrichment strategy for secondary prevention trials in Alzheimer disease. Alzheimer Dis Assoc Disord 2010;24:269–77.
[45] Holland D, McEvoy LK, Dale AM. Unbiased comparison of sample size estimates from longitudinal structural measures in ADNI. Hum Brain Mapp 2012;33:2586–602.
[46] Whitwell JL, Petersen RC, Negash S, Weigand SD, Kantarci K, Ivnik RJ, et al. Patterns of atrophy differ among specific subtypes of mild cognitive impairment. Arch Neurol 2007;64:1130–8.
[47] Aisen PS, Petersen RC, Donohue MC, Gamst A, Raman R, Thomas RG, et al. Clinical Core of the Alzheimer's Disease Neuroimaging Initiative: progress and plans. Alzheimers Dement 2010; 6:239–46.
[48] Stricker NH, Chang YL, Fennema-Notestine C, Delano-Wood L, Salmon DP, Bondi MW, et al. Distinct profiles of brain and cognitive changes in the very old with Alzheimer disease. Neurology 2011; 77:713–21.
[49] Holland D, Desikan RS, Dale AM, McEvoy LK. Higher rates of decline for women and apolipoprotein E epsilon4 carriers. AJNR Am J Neuroradiol 2013;34:2287–93.
[50] Holland D, McEvoy LK, Desikan RS, Dale AM. Enrichment and stratification for predementia Alzheimer disease clinical trials. PLoS One 2012;7:e47739.
[51] Jack CR Jr, Wiste HJ, Vemuri P, Weigand SD, Senjem ML, Zeng G, et al. Brain beta-amyloid measure and magnetic resonance imaging atrophy both predict time-to-progression from mild cognitive impairment to Alzheimer's disease. Brain 2010;133:3336–48.
[52] Chiang GC, Insel PS, Tosun D, Schuff N, Truran-Sacrey D, Raptentsetsang S, et al. Identifying cognitively healthy elderly individuals with subsequent memory decline by using automated MR temporoparietal volumes. Radiology 2011;259:844–51.
[53] Vemuri P, Wiste HJ, Weigand SD, Shaw LM, Trojanowski JQ, Weiner MW, et al. MRI and CSF biomarkers in normal, MCI, and AD subjects: predicting future clinical change. Neurology 2009; 73:294–301.
[54] Risacher SL, Shen L, West JD, Kim S, McDonald BC, Beckett LA, et al. Longitudinal MRI atrophy biomarkers: relationship to conversion in the ADNI cohort. Neurobiol Aging 2010;31:1401–18.
[55] Landau SM, Harvey D, Madison CM, Reiman EM, Foster NL, Aisen PS, et al. Comparing predictors of conversion and decline in mild cognitive impairment. Neurology 2010;75:230–8.
[56] Ewers M, Walsh C, Trojanowski JQ, Shaw LM, Petersen RC, Jack CR Jr, et al. Prediction of conversion from mild cognitive impairment to Alzheimer's disease dementia based upon biomarkers and neuropsychological test performance. Neurobiol Aging 2012; 33:1203–14.
[57] Lehmann M, Koedam EL, Barnes J, Bartlett JW, Barkhof F, Wattjes MP, et al. Visual ratings of atrophy in MCI: prediction of conversion and relationship with CSF biomarkers. Neurobiol Aging 2013;34:73–82.
[58] Hill DL, Schwarz AJ, Isaac M, Pani L, Vamvakas S, Hemmings R, et al. Coalition Against Major Diseases/European Medicines Agency biomarker qualification of hippocampal volume for enrichment of

clinical trials in predementia stages of Alzheimer's disease. Alzheimers Dement 2014;10:421–4293.
[59] Yu P, Sun J, Wolz R, Stephenson D, Brewer J, Fox NC, et al. Operationalizing hippocampal volume as an enrichment biomarker for amnestic mild cognitive impairment trials: effect of algorithm, test-retest variability, and cut point on trial cost, duration, and sample size. Neurobiol Aging 2014;35:808–18.
[60] Reuter M, Rosas HD, Fischl B. Highly accurate inverse consistent registration: a robust approach. Neuroimage 2010;53:1181–96.
[61] Roweis ST, Saul LK. Nonlinear dimensionality reduction by locally linear embedding. Science 2000;290:2323–6.
[62] Liu X, Tosun D, Weiner MW, Schuff N. Locally linear embedding (LLE) for MRI based Alzheimer's disease classification. Neuroimage 2013;83:148–57.
[63] Schuff N, Tosun D, Insel PS, Chiang GC, Truran D, Aisen PS, et al. Nonlinear time course of brain volume loss in cognitively normal and impaired elders. Neurobiol Aging 2012;33:845–55.
[64] Kantarci K, Xu Y, Shiung MM, O'Brien PC, Cha RH, Smith GE, et al. Comparative diagnostic utility of different MR modalities in mild cognitive impairment and Alzheimer's disease. Dement Geriatr Cogn Disord 2002;14:198–207.
[65] Fjell AM, Walhovd KB, Fennema-Notestine C, McEvoy LK, Hagler DJ, Holland D, et al. Brain atrophy in healthy aging is related to CSF levels of Abeta1-42. Cereb Cortex 2010;20:2069–79.
[66] Heister D, Brewer JB, Magda S, Blennow K, McEvoy LK. Predicting MCI outcome with clinically available MRI and CSF biomarkers. Neurology 2011;77:1619–28.
[67] Walhovd KB, Fjell AM, Brewer J, McEvoy LK, Fennema-Notestine C, Hagler DJ Jr, et al. Combining MR imaging, positron-emission tomography, and CSF biomarkers in the diagnosis and prognosis of Alzheimer disease. AJNR Am J Neuroradiol 2010; 31:347–54.
[68] Walhovd KB, Fjell AM, Dale AM, McEvoy LK, Brewer J, Karow DS, et al. Multi-modal imaging predicts memory performance in normal aging and cognitive decline. Neurobiol Aging 2010; 31:1107–21.
[69] Vemuri P, Wiste HJ, Weigand SD, Shaw LM, Trojanowski JQ, Weiner MW, et al. MRI and CSF biomarkers in normal, MCI, and AD subjects: diagnostic discrimination and cognitive correlations. Neurology 2009;73:287–93.
[70] Mattsson N, Insel PS, Donohue M, Landau S, Jagust WJ, Shaw LM, et al. Independent information from cerebrospinal fluid amyloid-beta and florbetapir imaging in Alzheimer's disease. Brain 2015;138(Pt 3):772–83.
[71] Desikan RS, McEvoy LK, Thompson WK, Holland D, Brewer JB, Aisen PS, et al. Amyloid-beta–associated clinical decline occurs only in the presence of elevated P-tau. Arch Neurol 2012;69:709–13.
[72] Desikan RS, McEvoy LK, Thompson WK, Holland D, Roddey JC, Blennow K, et al. Amyloid-beta associated volume loss occurs only in the presence of phospho-tau. Ann Neurol 2011;70:657–61.
[73] Desikan RS, Thompson WK, Holland D, Hess CP, Brewer JB, Zetterberg H, et al. Heart fatty acid binding protein and Abeta-associated Alzheimer's neurodegeneration. Mol Neurodegener 2013;8:39.
[74] Desikan RS, Thompson WK, Holland D, Hess CP, Brewer JB, Zetterberg H, et al. The role of clusterin in amyloid-beta-associated neurodegeneration. JAMA Neurol 2014;71:180–7.
[75] Insel PS, Mattsson N, Donohue MC, Mackin RS, Aisen PS, Jack CR Jr, et al. Alzheimer's Disease Neuroimaging I: the transitional association between beta-amyloid pathology and regional brain atrophy. Alzheimers Dement 2014.
[76] Mattsson N, Insel P, Donohue M, Jagust W, Sperling RA, Aisen PS, et al. Predicting reduction of CSF Aβ42 in cognitively healthy controls. JAMA Neurol 2015;72:554–60.
[77] Mattsson N, Insel PS, Nosheny R, Tosun D, Trojanowski JQ, Shaw LM, et al. Alzheimer's Disease Neuroimaging I: emerging beta-amyloid pathology and accelerated cortical atrophy. JAMA Neurol 2014;71:725–34.
[78] Chiang GC, Insel PS, Tosun D, Schuff N, Truran-Sacrey D, Raptentsetsang ST, et al. Impact of apolipoprotein varepsilon4-cerebrospinal fluid beta-amyloid interaction on hippocampal volume loss over 1 year in mild cognitive impairment. Alzheimers Dement 2011;7:514–20.
[79] Nosheny RL, Insel PS, Truran D, Schuff N, Jack CR Jr, Aisen PS, et al. Alzheimer's Disease Neuroimaging I: variables associated with hippocampal atrophy rate in normal aging and mild cognitive impairment. Neurobiol Aging 2015;36:273–82.
[80] Schott JM, Bartlett JW, Fox NC, Barnes J. Increased brain atrophy rates in cognitively normal older adults with low cerebrospinal fluid Abeta1-42. Ann Neurol 2010;68:825–34.
[81] Tosun D, Schuff N, Shaw LM, Trojanowski JQ, Weiner MW. Alzheimer's Disease NeuroImaging I: relationship between CSF biomarkers of Alzheimer's disease and rates of regional cortical thinning in ADNI data. J Alzheimers Dis 2011;26(Suppl 3): 77–90.
[82] Tosun D, Schuff N, Truran-Sacrey D, Shaw LM, Trojanowski JQ, Aisen P, et al. Relations between brain tissue loss, CSF biomarkers, and the ApoE genetic profile: a longitudinal MRI study. Neurobiol Aging 2010;31:1340–54.
[83] Mattsson N, Insel PS, Aisen PS, Jagust W, Mackin S, Weiner M, For the Alzheimer's Disease Neuroimaging Initiative. Brain structure and function as mediators of the effects of amyloid on memory. Neurology 2015;84:1136–44.
[84] Mattsson N, Tosun D, Insel PS, Simonson A, Jack CR Jr, Beckett LA, et al. Association of brain amyloid-beta with cerebral perfusion and structure in Alzheimer's disease and mild cognitive impairment. Brain 2014;137(Pt 5):1550–61.
[85] Tosun D, Schuff N, Mathis CA, Jagust W, Weiner MW. Spatial patterns of brain amyloid-beta burden and atrophy rate associations in mild cognitive impairment. Brain 2011;134(Pt 4):1077–88.
[86] Whitwell JL, Wiste HJ, Weigand SD, Rocca WA, Knopman DS, Roberts RO, et al. Comparison of imaging biomarkers in the Alzheimer Disease Neuroimaging Initiative and the Mayo Clinic Study of Aging. Arch Neurol 2012;69:614–22.
[87] Tosun D, Joshi S, Weiner MW. Neuroimaging predictors of brain amyloidosis in mild cognitive impairment. Ann Neurol 2013; 74:188–98.
[88] Tosun D, Joshi S, Weiner MW, the Alzheimer's Disease Neuroimaging Initiative. Multimodal MRI-based imputation of the Abeta+ in early mild cognitive impairment. Ann Clin Transl Neurol 2014; 1:160–70.
[89] Raj A, LoCastro E, Kuceyeski A, Tosun D, Relkin N, Weiner M, for the Alzheimer's Disease Neuroimaging Initiative. Network diffusion model of progression predicts longitudinal patterns of atrophy and metabolism in Alzheimer's disease. Cell Rep 2015;10:359–69.
[90] Mackin RS, Insel P, Tosun D, Mueller SG, Schuff N, Truran-Sacrey D, et al. The effect of subsyndromal symptoms of depression and white matter lesions on disability for individuals with mild cognitive impairment. Am J Geriatr Psychiatry 2013;21:906–14.
[91] Apostolova LG, Hwang KS, Andrawis JP, Green AE, Babakchanian S, Morra JH, et al. 3D PIB and CSF biomarker associations with hippocampal atrophy in ADNI subjects. Neurobiol Aging 2010;31:1284–303.
[92] Chou YY, Lepore N, Saharan P, Madsen SK, Hua X, Jack CR, et al. Ventricular maps in 804 ADNI subjects: correlations with CSF biomarkers and clinical decline. Neurobiol Aging 2010;31:1386–400.
[93] Rajagopalan P, Hua X, Toga AW, Jack CR Jr, Weiner MW, Thompson PM. Homocysteine effects on brain volumes mapped in 732 elderly individuals. Neuroreport 2011;22:391–5.
[94] Rajagopalan P, Toga AW, Jack CR, Weiner MW, Thompson PM. Fat-mass-related hormone, plasma leptin, predicts brain volumes in the elderly. Neuroreport 2013;24:58–62.

[95] Kohannim O, Hua X, Rajagopalan P, Hibar DP, Jahanshad N, Grill JD, et al. Multilocus genetic profiling to empower drug trials and predict brain atrophy. Neuroimage Clin 2013;2:827–35.
[96] Jack CR Jr, Knopman DS, Jagust WJ, Shaw LM, Aisen PS, Weiner MW, et al. Hypothetical model of dynamic biomarkers of the Alzheimer's pathological cascade. Lancet Neurol 2010;9:119–28.
[97] Jack CR Jr, Knopman DS, Jagust WJ, Petersen RC, Weiner MW, Aisen PS, et al. Tracking pathophysiological processes in Alzheimer's disease: an updated hypothetical model of dynamic biomarkers. Lancet Neurol 2013;12:207–16.
[98] Jack CR Jr, Vemuri P, Wiste HJ, Weigand SD, Lesnick TG, Lowe V, et al. Shapes of the trajectories of 5 major biomarkers of Alzheimer disease. Arch Neurol 2012;69:856–67.
[99] Jack CR Jr, Wiste HJ, Lesnick TG, Weigand SD, Knopman DS, Vemuri P, et al. Brain beta-amyloid load approaches a plateau. Neurology 2013;80:890–6.
[100] Bateman RJ, Xiong C, Benzinger TL, Fagan AM, Goate A, Fox NC, et al. Clinical and biomarker changes in dominantly inherited Alzheimer's disease. N Engl J Med 2012;367:795–804.
[101] Fagan AM, Xiong C, Jasielec MS, Bateman RJ, Goate AM, Benzinger TL, et al. Longitudinal change in CSF biomarkers in autosomal-dominant Alzheimer's disease. Sci Transl Med 2014;6:226ra230.
[102] Benzinger TL, Blazey T, Jack CR Jr, Koeppe RA, Su Y, Xiong C, et al. Regional variability of imaging biomarkers in autosomal dominant Alzheimer's disease. Proc Natl Acad Sci U S A 2013;110:E4502–9.
[103] Fleisher AS, Chen K, Quiroz YT, Jakimovich LJ, Gutierrez Gomez M, Langois CM, et al. Associations between biomarkers and age in the presenilin 1 E280A autosomal dominant Alzheimer disease kindred: a cross-sectional study. JAMA Neurol 2015;72:316–24.
[104] Jack CR Jr, Holtzman DM. Biomarker modeling of Alzheimer's disease. Neuron 2013;80:1347–58.
[105] Jedynak BM, Lang A, Liu B, Katz E, Zhang Y, Wyman BT, et al. A computational neruodegenerative disease progression score: method and results with the Alzheimer's disease neuroimaging initiative cohort. Neuroimage 2012;63:1478–86.
[106] Young AL, Oxtoby NP, Daga P, Cash DM, Fox NC, Ourselin S, et al. A data-driven model of biomarker changes in sporadic Alzheimer's disease. Brain 2014;137(Pt 9):2564–77.
[107] Caroli A, Frisoni GB. The dynamics of Alzheimer's disease biomarkers in the Alzheimer's Disease Neuroimaging Initiative cohort. Neurobiol Aging 2010;31:1263–74.
[108] Donohue MC, Jacqmin-Gadda H, Le Goff M, Thomas RG, Raman R, Gamst AC, et al. Estimating long-term multivariate progression from short-term data. Alzheimers Dement 2014;10(5 Suppl):S400–10.
[109] Jack CR Jr, Vemuri P, Wiste HJ, Weigand SD, Aisen PS, Trojanowski JQ, et al. Evidence for ordering of Alzheimer disease biomarkers. Arch Neurol 2011;68:1526–35.
[110] Jack CR Jr, Wiste HJ, Knopman DS, Vemuri P, Mielke MM, Weigand SD, et al. Rates of beta-amyloid accumulation are independent of hippocampal neurodegeneration. Neurology 2014;82:1605–12.
[111] Villemagne VL, Burnham S, Bourgeat P, Brown B, Ellis KA, Salvado O, et al. Amyloid beta deposition, neurodegeneration, and cognitive decline in sporadic Alzheimer's disease: a prospective cohort study. Lancet Neurol 2013;12:357–67.
[112] Jack CR Jr, Wiste HJ, Weigand SD, Knopman DS, Lowe V, Vemuri P, et al. Amyloid-first and neurodegeneration-first profiles characterize incident amyloid PET positivity. Neurology 2013;81:1732–40.
[113] Jack CR Jr, Wiste HJ, Weigand SD, Rocca WA, Knopman DS, Mielke MM, et al. Age-specific population frequencies of cerebral beta-amyloidosis and neurodegeneration among people with normal cognitive function aged 50-89 years: a cross-sectional study. Lancet Neurol 2014;13:997–1005.
[114] Jack CR Jr, Knopman DS, Weigand SD, Wiste HJ, vemuri P, Lowe V, et al. An operational approach to NIA-AA criteria for preclinical Alzheimer's disease. Ann Neurol 2012;71:765–75.
[115] Jack CR Jr, Wiste HJ, Weigand SD, Knopman DS, Vemuri P, Mielke MM, et al. Age, sex, and APOE epsilon4. Effects on memory, brain structure, and beta-amyloid across the adult life span. JAMA Neurol 2015;72:511–9.
[116] Dubois B, Feldman HH, Jacova C, Hampel H, Molinuevo JL, Blennow K, et al. Advancing research diagnostic criteria for Alzheimer's disease: the IWG-2 criteria. Lancet Neurol 2014;13:614–29.
[117] Albert MS, DeKosky ST, Dickson D, Dubois B, Feldman HH, Fox NC, et al. The diagnosis of mild cognitive impairment due to Alzheimer's disease: recommendations from the National Institute on Aging and Alzheimer's Association Workgroup. Alzheimers Dement 2011;7:270–9.
[118] McKhann GM, Knopman DS, Chertkow H, Hyman BT, Jack CR Jr, Kawas CH, et al. The diagnosis of dementia due to Alzheimer's disease: recommendations from the National Institute on Aging and the Alzheimer's Association Workgroup. Alzheimers Dement 2011;7:263–9.
[119] Jack CR Jr, Albert MS, Knopman DS, McKhann GM, Sperling RA, Carillo M, et al. Introduction to the recommendations from the National Institute on Aging-Alzheimer's Association workgroups on diagnostic guidelines for Alzheimer's disease. Alzheimers Dement 2011;7:257–62.
[120] Sperling RA, Aisen PS, Beckett LA, Bennett DA, Craft S, Fagan AM, et al. Toward defining the preclinical stages of Alzheimer's disease: recommendations from the National Institute on Aging-Alzheimer's Association workgroups on diagnostic guidelines for Alzheimer's disease. Alzheimers Dement 2011;7:280–92.
[121] Caroli A, Prestia A, Galluzzi S, Ferrari C, van der Flier WM, Ossenkoppele R, et al. Mild cognitive impairment with suspected nonamyloid pathology (SNAP): prediction of progression. Neurology 2015;84:508–15.
[122] Petersen RC, Aisen P, Boeve BF, Geda YE, Ivnik RJ, Knopman DS, et al. Criteria for mild cognitive impairment due to Alzheimer's disease in the community. Ann Neurol 2013;74(2):199–208.
[123] Toledo JB, Weiner MW, Wolk DA, Da X, Chen K, Arnold SE, et al. Neuronal injury biomarkers and prognosis in ADNI subjects with normal cognition. Acta Neuropathol Commun 2014;2:26.
[124] Lowe VJ, Peller PJ, Weigand SD, Montoya Quintero C, Tosakulwong N, Vemuri P, et al. Application of the National Institute on Aging-Alzheimer's Association AD criteria to ADNI. Neurology 2013;80:2130–7.
[125] Knopman DS, Jack CR Jr, Wiste HJ, Weigand SD, Vemuri P, Lowe V, et al. Short-term clinical outcomes for stages of NIA-AA preclinical Alzheimer disease. Neurology 2012;78:1576–82.
[126] Vos SJ, Xiong C, Visser PJ, Jasielec MS, Hassenstab J, Grant EA, et al. Preclinical Alzheimer's disease and its outcome: a longitudinal cohort study. Lancet Neurol 2013;12:957–65.
[127] Wirth M, Villeneuve S, Haase CM, Madison CM, Oh H, Landau SM, et al. Associations between Alzheimer disease biomarkers, neurodegeneration, and cognition in cognitively normal older people. JAMA Neurol 2013;70:1512–9.
[128] Mormino EC, Betensky RA, Hedden T, Schultz AP, Amariglio RE, Rentz DM, et al. Synergistic effect of beta-amyloid and neurodegeneration on cognitive decline in clinically normal individuals. JAMA Neurol 2014;71:1379–85.
[129] van Harten AC, Smits LL, Teunissen CE, Visser PJ, Koene T, Blankenstein MA, et al. Preclinical AD predicts decline in memory and executive functions in subjective complaints. Neurology 2013;81:1409–16.
[130] Prestia A, Caroli A, van der Flier WM, Ossenkoppele R, Van Berckel B, Barkhof F, et al. Prediction of dementia in MCI patients based on core diagnostic markers for Alzheimer disease. Neurology 2013;80:1048–56.

[131] Manning EN, Barnes J, Cash DM, Bartlett JW, Leung KK, Ourselin S, et al. APOE epsilon4 is associated with disproportionate progressive hippocampal atrophy in AD. PLoS One 2014; 9:e97608.
[132] Stein JL, Hua X, Morra JH, Lee S, Hibar DP, Ho AJ, et al. Genome-wide analysis reveals novel genes influencing temporal lobe structure with relevance to neurodegeneration in Alzheimer's disease. Neuroimage 2010;51:542–54.
[133] Hibar DP, Stein JL, Kohannim O, Jahanshad N, Saykin AJ, Shen L, et al. Voxelwise gene-wide association study (vGeneWAS): multivariate gene-based association testing in 731 elderly subjects. Neuroimage 2011;56:1875–91.
[134] Ho AJ, Stein JL, Hua X, Lee S, Hibar DP, Leow AD, et al. A commonly carried allele of the obesity-related FTO gene is associated with reduced brain volume in the healthy elderly. Proc Natl Acad Sci U S A 2010;107:8404–9.
[135] Stein JL, Hibar DP, Madsen SK, Khamis M, McMahon KL, de Zubicaray GI, et al. Discovery and replication of dopamine-related gene effects on caudate volume in young and elderly populations (N=1198) using genome-wide search. Mol Psychiatry 2011; 16:927–37. 881.
[136] Roussotte FF, Jahanshad N, Hibar DP, Sowell ER, Kohannim O, Barysheva M, et al. A commonly carried genetic variant in the delta opioid receptor gene, OPRD1, is associated with smaller regional brain volumes: replication in elderly and young populations. Hum Brain Mapp 2014;35:1226–36.
[137] Rajagopalan P, Jahanshad N, Stein JL, Hua X, Madsen SK, Kohannim O, et al. Common folate gene variant, MTHFR C677T, is associated with brain structure in two independent cohorts of people with mild cognitive impairment. Neuroimage Clin 2012; 1:179–87.
[138] Rajagopalan P, Hibar DP, Thompson PM. TREM2 and neurodegenerative disease. N Engl J Med 2013;369:1565–7.
[139] Hibar DP, Stein JL, Renteria ME, Arias-Vasquez A, Desrivieres S, Jahanshad N, et al. Common genetic variants influence human subcortical brain structures. Nature 2015;520:224–9.
[140] Jack CR Jr, Barkhof F, Bernstein MA, Cantillon M, Cole PE, Decarli C, et al. Steps to standardization and validation of hippocampal volumetry as a biomarker in clinical trials and diagnostic criterion for Alzheimer's disease. Alzheimers Dement 2011;7:474–4854.
[141] Frisoni GB, Jack CR, Bocchetta M, Bauer C, Frederiksen KS, Liu Y, et al. The EADC-ADNI Harmonized Protocol for manual hippocampal segmentation on magnetic resonance: evidence of validity. Alzheimers Dement 2014;11:111–25.
[142] Boccardi M, Ganzola R, Bocchetta M, Pievani M, Redolfi A, Bartzokis G, et al. Survey of protocols for the manual segmentation of the hippocampus: preparatory steps towards a joint EADC-ADNI harmonized protocol. J Alzheimers Dis 2011;26(Suppl 3):61–75.
[143] Bocchetta M, Boccardi M, Ganzola R, Apostolova LG, Preboske G, Wolf D, et al. Harmonized benchmark labels of the hippocampus on magnetic resonance: the EADC-ADNI project. Alzheimers Dement 2014;11:151–1605.
[144] Schneider JA, Arvanitakis Z, Bang W, Bennett DA. Mixed brain pathologies account for most dementia cases in community-dwelling older persons. Neurology 2007;69:2197–204.
[145] Schwarz C, Fletcher E, DeCarli C, Carmichael O. Fully-automated white matter hyperintensity detection with anatomical prior knowledge and without FLAIR. Inf Process Med Imaging 2009;21:239–51.
[146] Carmichael O, Schwarz C, Drucker D, Fletcher E, Harvey D, Beckett L, et al. Longitudinal changes in white matter disease and cognition in the first year of the Alzheimer disease neuroimaging initiative. Arch Neurol 2010;67:1370–8.
[147] Barnes J, Carmichael OT, Leung KK, Schwarz C, Ridgway GR, Bartlett JW, et al. Vascular and Alzheimer's disease markers independently predict brain atrophy rate in Alzheimer's Disease Neuroimaging Initiative controls. Neurobiol Aging 2013;34:1996–2002.
[148] Haight TJ, Landau SM, Carmichael O, Schwarz C, DeCarli C, Jagust WJ. Dissociable effects of Alzheimer disease and white matter hyperintensities on brain metabolism. JAMA Neurol 2013;70: 1039–45.
[149] Lo RY, Jagust WJ. Vascular burden and Alzheimer disease pathologic progression. Neurology 2012;79:1349–55.
[150] DeCarli C. Clinically asymptomatic vascular brain injury: a potent cause of cognitive impairment among older individuals. J Alzheimers Dis 2013;33(Suppl 1):S417–26.
[151] Nettiksimmons J, Beckett L, Schwarz C, Carmichael O, Fletcher E, Decarli C. Subgroup of ADNI normal controls characterized by atrophy and cognitive decline associated with vascular damage. Psychol Aging 2013;28:191–201.
[152] Nettiksimmons J, DeCarli C, Landau S, Beckett L. Biological heterogeneity in ADNI amnestic mild cognitive impairment. Alzheimers Dement 2014;10(5):511–5211.
[153] Nettiksimmons J, Harvey D, Brewer J, Carmichael O, DeCarli C, Jack CR Jr, et al. Subtypes based on cerebrospinal fluid and magnetic resonance imaging markers in normal elderly predict cognitive decline. Neurobiol Aging 2010;31:1419–28.
[154] Morris JC, Storandt M, Miller JP, McKeel DW, Price JL, Rubin EH, et al. Mild cognitive impairment represents early-stage Alzheimer disease. Arch Neurol 2001;58:397–405.
[155] Vemuri P, Weigand SD, Przybelski SA, Knopman DS, Smith GE, Trojanowski JQ, et al. Cognitive reserve and Alzheimer's disease biomarkers are independent determinants of cognition. Brain 2011; 134(Pt 5):1479–92.
[156] Sperling R, Salloway S, Brooks DJ, Tampieri D, Barakos J, Fox NC, et al. Amyloid-related imaging abnormalities in patients with Alzheimer's disease treated with bapineuzumab: a retrospective analysis. Lancet Neurol 2012;11:241–9.
[157] Salloway S, Sperling R, Gilman S, Fox NC, Blennow K, Raskind M, et al. A phase 2 multiple ascending dose trial of bapineuzumab in mild to moderate Alzheimer disease. Neurology 2009;73:2061–70.
[158] Kantarci K, Gunter JL, Tosakulwong N, Weigand SD, Senjem MS, Petersen RC, et al. Focal hemosiderin deposits and beta-amyloid load in the ADNI cohort. Alzheimers Dement 2013;9(5 Suppl): S116–23.
[159] Tosun D, Schuff N, Weiner M. An integrated multimodality MR brain imaging study: gray matter tissue loss mediates the association between cerebral hypoperfusion and Alzheimer's disease. Conf Proc IEEE Eng Med Biol Soc 2009;2009:6981–4.
[160] Tosun D, Mojabi P, Weiner MW, Schuff N. Joint analysis of structural and perfusion MRI for cognitive assessment and classification of Alzheimer's disease and normal aging. Neuroimage 2010;52:186–97.
[161] ISBI: 2014; Brooklyn, NY, USA; 2014.
[162] Nir TM, Jahanshad N, Villalon-Reina JE, Toga AW, Jack CR, Weiner MW, et al. Effectiveness of regional DTI measures in distinguishing Alzheimer's disease, MCI, and normal aging. Neuroimage Clin 2013;3:180–95.
[163] Nir TM, Jahanshad N, Toga AW, Bernstein MA, Jack CR Jr, Weiner MW, et al. Connectivity network measures predict volumetric atrophy in mild cognitive impairment. Neurobiol Aging 2015; 36(Suppl 1):S113–20.
[164] Nir TM, Villalon-Reina JE, Prasad G, Jahanshad N, Joshi SH, Toga AW, et al. Diffusion weighted imaging-based maximum density path analysis and classification of Alzheimer's disease. Neurobiol Aging 2015;36(Suppl 1):S132–40.
[165] Prasad G, Joshi SH, Nir TM, Toga AW, Thompson PM. Brain connectivity and novel network measures for Alzheimer's disease classification. Neurobiol Aging 2015;36(Suppl 1):S121–31.
[166] Prasad G, Nir TM, Toga AW, Thompson PM. Tractography density and network measures in Alzheimer's disease. Proc IEEE Int Symp Biomed Imaging 2013;2013:692–5.
[167] Prasad G, Joshi SH, Nir TM, Toga AW, Thompson PM. Flow-based network measures of brain connectivity in Alzheimer's disease. Proc IEEE Int Symp Biomed Imaging 2013;2013:258–61.

[168] ISBI: 2015; Brooklyn, NY, USA; 2015.
[169] Zhan L, Zhi N, Jin Y, Wang Y, Jahanshad N, Prasad G, et al. Multiple stages classification of Alzheimer's disease based on structural brain networks using Generalized Low Rank Approximations (GLRAM). In: MICCAI CDMRI Workshop. Boston, MA, USA: Springer; 2014.
[170] Daianu M, Dennis EL, Jahanshad N, Nir TM, Toga AW, Jack CR Jr, et al. Disrupted brain connectivity in Alzheimer's disease: effects of network thresholding. In: Computational diffusion MRI and brain connectivity (MICCAI BC Workshop); 2013;. p. 199–208. Japan.
[171] Daianu M, Dennis EL, Jahanshad N, Nir TM, Toga AW, Jack CR Jr, et al. Alzheimer's disease disrupts rich club organization in brain connectivity networks. Proc IEEE Int Symp Biomed Imaging 2013;:266–9.
[172] Daianu M, Jahanshad N, Nir TM, Toga AW, Jack CR Jr, Weiner MW, et al. Breakdown of brain connectivity between normal aging and Alzheimer's disease: a structural k-core network analysis. Brain Connect 2013;3:407–22.
[173] Daianu M, Jahanshad N, Nir TM, Leonardo CD, Jack CR Jr, Weiner M, et al. Algebraic connectivity of brain networks shows patterns of segregation leading to reduced network robustness in Alzheimer's disease. In: MICCAI CDMRI. Boston, MA, USA: Springer; 2014.
[174] Zhan L, Bernstein M, Borowski BJ, Jack CR Jr, Thompson P. Evaluation of diffusion imaging protocols for the Alzheimer's Disease Neuroimaging Initiative. In: 2014 IEEE 11th International Symposium on Biomedical Imaging (ISBI). Beijing, China: IEEE; 2014. p. 710–3.
[175] Zhan L, Jahanshad N, Jin Y, Nir TM, Leonardo CD, Bernstein M, et al. Understanding scanner upgrade effects on brain integrity and connectivity measures. In: 2014 IEEE 11th International Symposium Biomedical Imaging (ISBI). Beijing, China: IEEE; 2014. p. 234–7.
[176] 2014 IEEE 11th International Symposium on Biomedical Imaging (ISBI): 2014 Beijing, China: IEEE; 2014. p. 1027–30.
[177] Warstadt NM, Dennis EL, Jahanshad N, Kohannim O, Nir TM, McMahon KL, et al. Serum cholesterol and variant in cholesterol-related gene CETP predict white matter microstructure. Neurobiol Aging 2014;35:2504–13.
[178] Jahanshad N, Bhatt P, Hibar DP, Villalon-Reina JE, Nir TM, Toga AW, et al. Bivariate genome-wide association study of genetically correlated neuroimaging phenotypes from DTI and MRI through a seemingly unrelated regression model. In: MICCAI; 2013;. p. 189–201. Nagoya, Japan.
[179] Jahanshad N, Kochunov P, Glahn DC, Blangero J, Nichols TE, McMahon KL, et al. Power estimates for voxel-based genetic association studies using diffusion imaging. In: MICCAI; 2013;. p. 229–38. Nagoya, Japan.
[180] Jones DT, Vemuri P, Murphy MC, Gunter JL, Senjem ML, Machulda MM, et al. Non-stationarity in the "resting brain's" modular architecture. PLoS One 2012;7:e39731.